University of Sistan and Baluchestan

Journal of Epigenetics

Online ISSN: 2676 - 4350

Homepage: https://jep.usb.ac.ir

Iranian Genetics Society

Effect of Zinc Oxide Nanoparticles Conjugated with Safranal on MMP1 and mTOR Gene Expression in MCF-7 Breast Cancer Cells

Reihanneh Jassemnejad [1], Amir Jalali [2*], Seyed Ataollah Sadat Shandiz [3], Ali Salehzadeh [4], Leila Kohan [5]

[1] Department of Biology, Ars. C., Islamic Azad University, Arsanjan, Iran. E-mail: rjassemnejad@gmail.com

[2] *Corresponding author*, Department of Biology, Faculty of Science, Arak University, Arak, Iran. E-mail: a-jalali@araku.ac.ir

[3] Department of Biology, CT. C., Islamic Azad University, Tehran, Iran. E-mail: ata.sadatshandiz@iauctb.ac.ir

[4] Department of Biology, Ra. C., Islamic Azad University, Rasht, Iran. E-mail: salehzadeh@iaurasht.ac.ir

[5] Department of Biology, Ars. C., Islamic Azad University, Arsanjan, Iran. E-mail: leila_kohan@yahoo.com

ARTICLE INFO

Article type:
Research Article

Article history:
Received:9 June 2025
Revised:6 July 2025
Accepted:6 September 2025

Keywords:
Breast Neoplasms,
Gene Expression,
Nanoparticles,
Safranal,
Zinc Oxide.

A B S T R A C T

Breast cancer is a leading cause of cancer-related mortality worldwide. Recent studies suggest that nanoparticles can enhance therapeutic efficacy. This research investigates the effects of zinc oxide nanoparticles (ZnO NPs) conjugated with Safranal on the expression of key genes associated with metabolism in Michigan Cancer Foundation (MCF-7) breast cancer cell lines. ZnO@Glu-Safranal NPs were synthesized and characterized using FE-SEM, transmission electron microscope (TEM), FT-IR, XRD, and Zeta potential analysis. To assess the effects of ZnO@Glu-Safranal NPs on the expression of MMP1 and mTOR genes, the MCF-7 cell line was treated with the IC50 concentration of the nanoparticles (165 µg/mL) for 24 hours, while untreated cells were used as a control. Changes in gene expression levels were quantified using real-time PCR, and $p < 0.05$ was considered statistically significant. The results showed decreased expression of MMP1 (0.87-fold, $p = 0.02$) and mTOR (0.86-fold, $p = 0.03$) in MCF-7 cell lines compared to the control group. The study demonstrates that ZnO@Glu-Safranal NPs effectively modulate the expression of key metabolic genes expression in breast cancer cell lines. These findings highlight their potential as an effective therapeutic strategy, emphasizing the need for further research into their mechanisms and clinical applications to enhance breast cancer treatment outcomes.

Introduction

Breast cancer remains one of the most prevalent malignancies among women worldwide, posing significant health challenges. It is characterized by uncontrolled proliferation of breast cells leading to tumor formation. The pathophysiology of breast cancer involves complex interactions between genetic, environmental, and lifestyle factors (Rudolph et al., 2016).

Matrix Metalloproteinase 1 (*MMP1*), located on chromosome 11q22.2-22.3, encodes a zinc-dependent endopeptidase responsible for degrading collagen. MMP1 plays a critical role in tissue remodeling and wound healing but is frequently overexpressed in cancer, facilitating tumor invasion and metastasis through extracellular matrix degradation (Puente et al., 2003). Clinical studies have demonstrated significantly elevated MMP1 levels in breast

DOI: https://doi.org/ 10.22111/JEP.2025.52363.1092

Publisher: University of Sistan and Baluchestan

How to Cite: Jassemnejad, R., Jalali, A., Shandiz, A., Salehzadeh, A., & Kohan, L. (2025). Effect of Zinc Oxide Nanoparticles Conjugated with Safranal on MMP1 and mTOR Gene Expression in MCF-7 Breast Cancer Cells. *Journal of Epigenetics*, 6(2), 27-38. https://doi.org/ 10.22111/JEP.2025.52363.1092

cancer tissues, correlating with poorer overall survival, particularly in grade II, nodal-negative, ER-positive, and HER2-negative patient subgroups. Thus, MMP1 serves as both a vital prognostic marker and a potential therapeutic target (Wang et al., 2017).

The mechanistic target of rapamycin (*mTOR*), encoded on chromosome 1p36.22, is a key kinase regulating cell growth and survival by integrating signals from nutrients and growth factors to control metabolism and cell cycle progression. Dysregulation of the *mTOR* pathway is common in many cancers, leading to uncontrolled cellular proliferation, which has made mTOR inhibitors promising candidates for targeted cancer therapy (Liu et al., 2017).

Nanotechnology has emerged as a promising field in cancer treatment, offering novel drug delivery systems and enhanced therapeutic efficacy (Al-Thani et al., 2024). Zinc oxide nanoparticles (ZnO NPs) have attracted considerable attention due to their biocompatibility, antibacterial properties, and potential anticancer effects (Sirelkhatim et al., 2015; Anjum et al., 2021). These nanoparticles induce oxidative stress in tumor cells by generating reactive oxygen species (ROS), leading to cellular damage and apoptosis (Wang et al., 2014; Bai et al., 2017; Li et al., 2020). Furthermore, conjugation of ZnO NPs with organic compounds such as porphyrin (Zhang et al., 2008), chitosan (Mohamed et al., 2024), ferulic acid (Ezhuthupurakkal et al., 2018), and chemotherapeutic agents like doxorubicin (Mishra et al., 2022) and methotrexate (Mishra et al., 2024) has been shown to enhance their cytotoxic effects and improve drug targeting.

Safranal, a natural monoterpenoid aldehyde ($C_{10}H_{14}O$) derived from the dried stigmas of Crocus sativus (saffron), is primarily responsible for saffron's distinctive aroma and flavor. Traditionally used in medicine, safranal has recently gained interest for its anticancer properties. Malaekeh-Nikouei et al. (2013) reported concentration-dependent cytotoxic effects of safranal on HeLa and MCF-7 cell lines, with enhanced efficacy observed in liposomal formulations. Samarghandian et al. (2014) demonstrated that safranal inhibits neuroblastoma cell growth in a dose- and time-dependent manner. Additionally, safranal exhibited chemopreventive effects in diethylnitrosamine (DEN)-induced liver cancer models by inhibiting cell proliferation, inducing apoptosis, and reducing inflammatory markers (Abdalla et al., 2022). Mechanistic studies by Naghshineh et al. (2015) revealed that safranal disrupts microtubule polymerization, suggesting its potential as a novel anticancer agent.

Most existing studies have focused on either the effects of ZnO nanoparticles or the pharmacological properties of safranal individually. However, to the best of our knowledge, the combined effects of ZnO nanoparticles conjugated with safranal (ZnO@Glu-Safranal) have not been investigated, representing a critical gap in current knowledge. This study aims to address this gap by evaluating the impact of ZnO@Glu-Safranal nanoparticles on the expression of key metabolic genes in MCF-7 breast cancer cells. By targeting crucial genes involved in cancer development and progression, this research proposes a novel therapeutic approach that integrates nanotechnology with natural bioactive compounds. The findings may provide valuable insights for developing more targeted and effective cancer therapies, thereby advancing the field of precision oncology.

Materials and Methods

Synthesis of Zinc Oxide Nanoparticles (ZnO NPs)

To prepare a 10 mM solution, zinc nitrate [$Zn(NO_3)_2$] (Sigma-Aldrich) was dissolved in 100 mL of distilled water. This solution was heated to 80 °C for 60 minutes, after which sodium hydroxide (NaOH) was added dropwise to adjust the pH to 12.0. The synthesis of ZnO NPs occurred by maintaining the $Zn(NO_3)_2$ solution at 100 °C. Subsequently, one gram of the dried ZnO NPs was mixed with 500 mg of D-Glucose in distilled water, sonicated for 30 minutes, and then heated at 180 °C for three hours to produce glucose-functionalized ZnO NPs (ZnO@Glu NPs). For conjugation with Safranal, one gram of ZnO@Glu NPs and 100 mg of Safranal (Sigma-Aldrich) were suspended in distilled water and shaken for 20 hours at room temperature. Finally, the resulting ZnO@Glu-Safranal NPs were collected and freeze-dried (Tajmehri et al., 2024).

Characterization of ZnO@Glu-Safranal Nanoparticles

After synthesizing the ZnO@Glu-Safranal NPs, various techniques were employed to analyze their physical and chemical properties. Given that the size and shape of nanoparticles directly influence their cellular uptake, the dimensions, morphology,

surface characteristics, and chemical composition of the synthesized nanoparticles were determined using a Scanning Electron Microscope (TESCAN MIRA3 FEG SEM, Czech Republic) equipped with an energy dispersive X-ray spectrometer and a Transmission Electron Microscope (Zeiss 900 EM, Carl Zeiss Inc., Oberköchen, Germany). To identify functional groups, characterize surface chemistry, and monitor chemical reactions, Fourier-transform infrared (FT-IR) spectroscopy was utilized. The FT-IR spectra of the samples were measured in potassium bromide (KBr) pellet form over the range of 4500–450 cm^{-1} using a Perkin Elmer Spectrum 100 FT-IR instrument. For assessing the purity and crystalline structure of the synthesized nanoparticles, Powder X-ray diffraction (PXRD) data were obtained using a Philips powder diffractometer (type PW1730, Cu-Kα X-radiation, λ = 1.54 Å). Additionally, a Zeta potential analyzer (Zetasizer Ver. 6.32, Malvern Instruments Ltd) was employed to evaluate the stability and surface charge of the nanoparticles.

Effects of ZnO@Glu-Safranal Nanoparticles on Cell Viability

The cytotoxicity and antiproliferative effects of ZnO@Glu-Safranal NPs were evaluated in treated and untreated MCF-7 cell lines using the MTT assay. Cell lines were sourced from the Pasteur Institute of Iran and cultured in RPMI1640 medium with 10% fetal bovine serum at 37 °C. A monolayer was established in 96-well plates, with a cell density of 1×10^4 cells per well. Various concentrations of the nanoparticles (7.8 to 1000 µg/mL) were added, while untreated wells served as controls. The cells were incubated for 24 hours in a 5% CO_2 atmosphere. Following incubation, 200 µL of MTT solution was added to each well, and the plates were further incubated at 37 °C for 4 hours. After removing the medium, 200 µL of DMSO was added to dissolve the formazan crystals, and absorbance was measured at 570 nm using a microplate reader. The percentage of cell survival was determined using the following formula:

$$\text{Survival percentage} = \frac{\text{OD570 of treated wells}}{\text{OD570 of untreated wells}} \times 100$$

Impact of ZnO@Glu-Safranal Nanoparticles on Gene Expression

The effect of ZnO@Glu-Safranal nanoparticles on the expression of metabolic genes in MCF-7 and control cells was evaluated using quantitative real-time polymerase chain reaction (qRT-PCR) following a 24-hour treatment with the IC_{50} concentration of the nanoparticles. Total RNA was extracted from cell samples with TriZol reagent and treated with DNase I to remove residual DNA. RNA concentration was measured using a Nano-Drop ND 1000 Spectrophotometer (Wilmington, USA). Reverse transcription was performed to synthesize cDNA using the SinaClon cDNA synthesis kit (Iran). The qRT-PCR analysis was conducted in triplicate with gene-specific primers (Table 1), and *GAPDH* was used as an internal control gene for normalization. The relative expression levels of the target genes were calculated using the $2^{-\Delta\Delta C_T}$ method. Each reaction mixture comprised 10 µl, including 1 µl of cDNA (100 µg/ml) as the template, 1 µl of SYBR Green Premix Ex TaqTM (TaKaRa, Japan), 0.6 µl of both primers (5µM), and 6.8 µl of diethylpyrocarbonate-treated water. The cycling conditions included an initial denaturation at 95 °C for 10 minutes, followed by 40 cycles consisting of 10 seconds at 95 °C, 15 seconds at 60 °C, and 20 seconds at 72 °C.

Table 1- Gene-specific primer sequences for qRT-PCR.

Primer	Sequence (5′ → 3′)	Target Size (bp)
MMP1-Forward	ATGAAGCAGCCCAG ATGTGGAG	137
MMP1-Reverse	TGGTCCACATCTGCT CTTGGCA	
mTOR-Forward	AGCATCGGATGCTTA GGAGTGG	146
mTOR-Reverse	CAGCCAGTCATCTTT GGAGACC	
GAPDH-Forward	GTCTCCTCTGACTTC AACAGCG	131
GAPDH-Reverse	ACCACCCTGTTGCTG TAGCCAA	

Statistical Analysis

For the statistical analysis, one-way ANOVA was performed using GraphPad Prism software (version 9.0). Experiments were conducted in triplicate, and *p*-values less than 0.05 were considered statistically significant.

Results

Nanoparticles Characterization

The successful conjugation of safranal to zinc oxide nanoparticles (ZnO NPs) was rigorously confirmed using Fourier-transform infrared (FT-IR) spectroscopy, providing molecular-level insights into the chemical interactions responsible for the enhanced biological activity of the conjugated nanoparticles (Fig. 1).

The FT-IR spectrum of ZnO NPs (Fig. 1a) revealed several characteristic peaks consistent with the wurtzite crystalline structure. A broad absorption band at 3422 cm^{-1} corresponds to O–H stretching vibrations, attributed to surface hydroxyl groups such as alcohols, phenols, or carboxylic acids. Peaks at 2924 cm^{-1} and 2857 cm^{-1} are assigned to C–H stretching vibrations of aliphatic hydrocarbons. Carbonyl-related C=O stretching vibrations appear at 1695 cm^{-1} and 1617 cm^{-1}, while C–H bending modes are observed at 1515 cm^{-1}, 1413 cm^{-1}, and 1388 cm^{-1}. Additionally, absorptions at 1230 cm^{-1} and 1023 cm^{-1} indicate C–O stretching from esters, ethers, or alcohols. These features collectively confirm the presence of surface functional groups and residual organic species from synthesis, consistent with previous reports (Sirelkhatim et al., 2015).

The FT-IR spectrum of pure safranal (Fig. 1b) displayed a broad O–H stretching peak at 3440 cm^{-1} and a C–H stretching peak at 2927 cm^{-1}, characteristic of aliphatic hydrocarbons. The carbonyl C=O stretch of the α, β-unsaturated aldehyde moiety appeared at 1695 cm^{-1}, accompanied by C=C stretching vibrations at 1615 cm^{-1}. C–H bending vibrations at 1515 cm^{-1}, 1413 cm^{-1}, and 1388 cm^{-1}, as well as C–O stretching peaks at 1230 cm^{-1} and 1023 cm^{-1}, further confirmed the molecular structure of safranal.

The FT-IR spectrum of the conjugated ZnO@Glu-Safranal nanoparticles (Fig. 1c) exhibited notable spectral modifications indicative of successful chemical conjugation. The O–H stretching band appeared slightly shifted and reduced in intensity at 3425 cm^{-1}, suggesting consumption of hydroxyl groups during conjugation. The aliphatic C–H stretching peak was observed at 2928 cm^{-1}, consistent with both ZnO and safranal components. Importantly, the carbonyl C=O stretching peak exhibited a redshift from 1695 cm^{-1} to 1685 cm^{-1}, indicating covalent modification of safranal's aldehyde group. A new peak at 1555 cm^{-1} was detected, attributed to C=N stretching vibrations, confirming Schiff base formation via glutaraldehyde crosslinking. Additional peaks at 1398 cm^{-1}, 1275 cm^{-1}, and 1035 cm^{-1} correspond to C–H bending and C–O stretching from various functional groups.

The preservation of Zn–O lattice vibrations below 1000 cm^{-1} (not explicitly detailed here but consistent with ZnO structure) confirms that the crystalline ZnO core remains intact post-conjugation. The covalent bonding mechanism, evidenced by the appearance of C=N bonds and the redshift in C=O stretching, ensures stable attachment of safranal to the nanoparticle surface, which is critical for effective and sustained therapeutic delivery. Furthermore, the retention of carbonyl groups (1685 cm^{-1}) may facilitate reactive oxygen species (ROS) generation, contributing to the observed enhanced anticancer effects in biological assays.

This comprehensive FT-IR analysis not only validates the successful synthesis of ZnO@Glu-Safranal nanoparticles but also provides mechanistic understanding of their improved therapeutic performance compared to unconjugated components. The chemical stability and defined molecular interactions revealed by these spectral features support the translational potential of this nanoconjugate in cancer therapy.

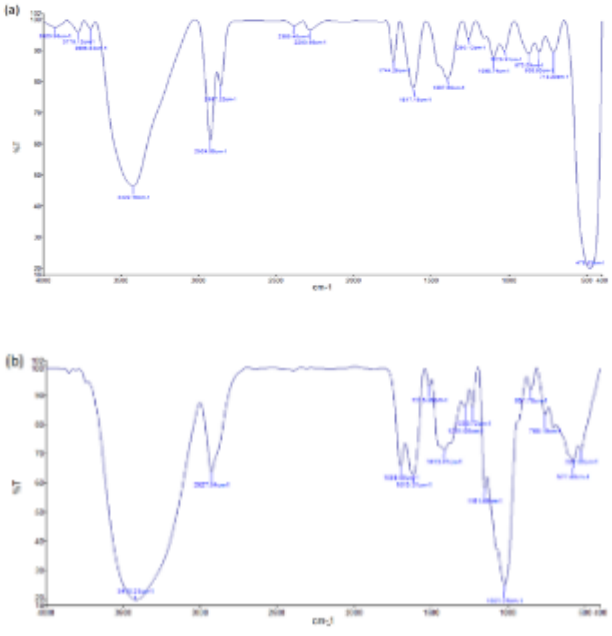

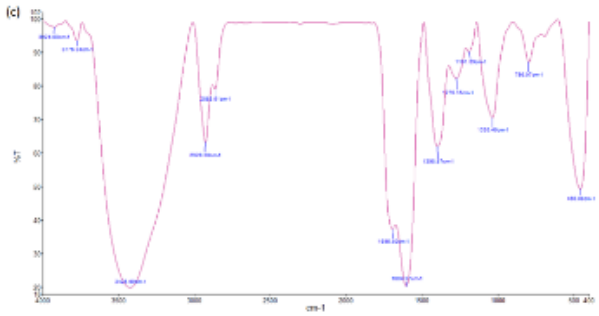

Fig. 1 – FT-IR spectrum of a) ZnO nanoparticles; b) Safranal, and c) ZnO@Glu-Safranal nanoparticles.

The X-ray diffraction pattern of ZnO@Glu-Safranal nanoparticles (Fig. 2) reveals a highly crystalline structure corresponding to the hexagonal wurtzite phase of ZnO (JCPDS No. 36-1451). The characteristic diffraction peaks observed at 31.76° (100), 34.42° (101), 36.32° (002), 47.54° (102), 56.60° (110), 62.86° (103), 66.38° (200), 67.96° (112), and 69.10° (201) confirm the successful synthesis of phase-pure ZnO nanoparticles without detectable impurities. The most intense peak at 36.32°, corresponding to the (002) plane, demonstrates the preferential growth orientation of the nanoparticles, with a calculated d-spacing of 2.471 Å that matches well with standard values for wurtzite ZnO.

Crystallite size analysis using the Scherrer equation applied to the (002) peak yields an average crystallite size of approximately 18 nm, based on the measured full width at half maximum (FWHM) of 0.45°. The narrow peak width indicates good crystallinity, while variations in peak broadening among different diffraction planes suggest a distribution of crystallite sizes within the sample. The presence of broader peaks at higher angles, particularly for the (102) plane at 47.54°, may indicate the existence of smaller crystallites or surface defects that could enhance the nanoparticles' reactivity and drug-loading capacity.

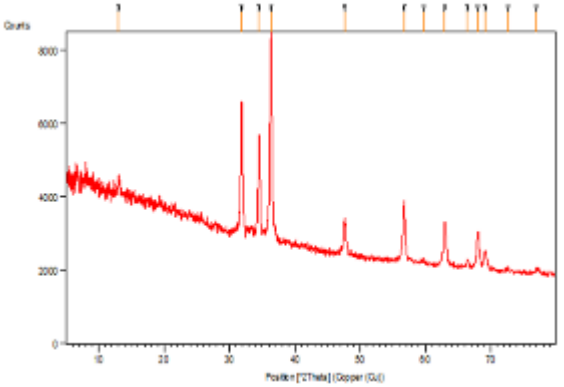

Fig. 2 - The X-ray diffraction analysis of the synthesized ZnO@Glu-Safranal nanoparticles.

The transmission electron microscopy (TEM) image (Fig. 3a) reveals well-dispersed ZnO@Glu-Safranal nanoparticles (NPs) exhibiting a spherical to oval morphology, with diameters ranging from 25 to 35 nm as determined by direct measurement. This size range is consistent with the crystallite size of 18 nm calculated from X-ray diffraction (XRD) data using the Scherrer equation. The observed 10-15% size difference between TEM measurements (representing individual particles) and XRD results (reflecting crystalline domains) suggests the presence of polycrystalline nanostructures, where each particle comprises multiple crystalline domains. The inset of Fig. 3a, showing selected-area electron diffraction, further confirms the wurtzite structure of the NPs, with diffraction patterns aligning with the XRD peak positions.

The field emission scanning electron microscopy (FE-SEM) image (Fig. 3b) displays uniform NPs with sizes ranging from 42 to 62 nm, which are slightly larger than those observed in TEM. This discrepancy can be attributed to several factors: the conductive coating required for SEM imaging, approximately 5 nm of Au/Pd; the presence of a Safranal-glutaraldehyde shell, as corroborated by the C=N peak in FT-IR spectra; and mild aggregation occurring during sample preparation. The spherical morphology observed in FE-SEM is consistent with the dominant (002) plane orientation identified in XRD, a configuration

known to minimize surface energy in wurtzite structures. The narrow size distribution, with SEM measurements (42-62 nm) encompassing the TEM core sizes (25-35 nm), underscores the successful conjugation of the NPs while preserving their structural integrity, as evidenced by the unchanged XRD peak positions following functionalization.

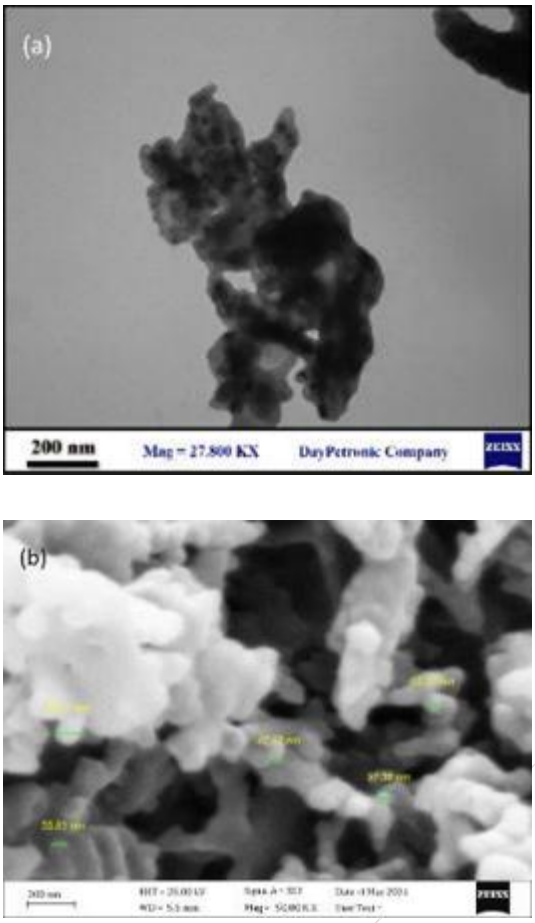

Fig. 3 - a) TEM; and b) FE-SEM image of the ZnO@Glu-Safranal nanoparticles.

The ZnO@Glu-Safranal NPs, with a zeta potential of -17 mV (Fig 4), exhibit moderate stability, suggesting potential for targeting cancer cells. This negative surface charge may enhance interactions with positively charged cellular membranes, facilitating uptake. However, the moderate zeta potential also indicates a risk of aggregation, which could hinder effective delivery. To optimize their therapeutic efficacy against cancer cell proliferation, further modifications may be needed to improve their surface properties and enhance cellular penetration.

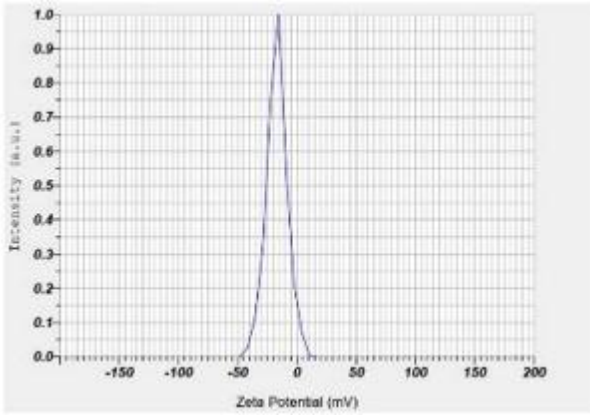

Fig. 4 - Zeta Potential Analysis of ZnO@Glu-Safranal Nanoparticles.

Cell viability assay

After a 24-hour exposure to the ZnO@Glu-Safranal NPs, the IC_{50} concentration for MCF-7 cells was found to be 165 µg/mL. Notably, a significant decrease in the viability of cancer cells was observed starting at a concentration of 31.25 µg/mL, with the effect becoming more pronounced as the concentration increased (Fig. 5).

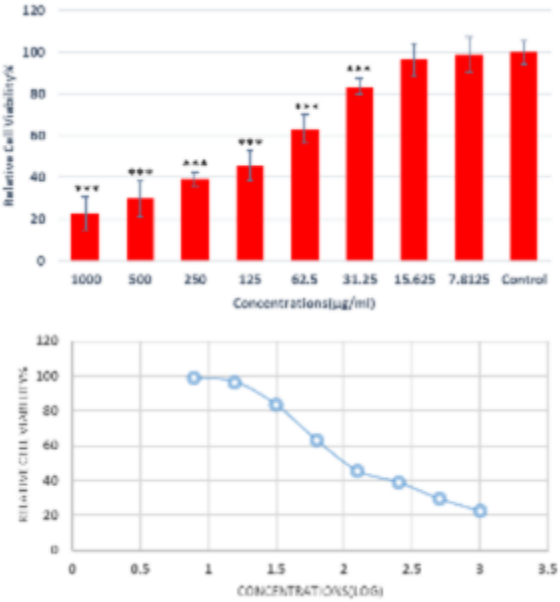

Fig. 5 - The toxicological effects of various concentrations of ZnO@Glu-Safranal nanoparticles (ranging from 7.8 to 1000 µg/mL) were assessed using the MTT assay after a 24-hour exposure on the MCF-7 cell line. The results are presented in comparison to control samples (n = 3, ***: P < 0.001).

Gene Expression Analysis

The results indicate that treatment with ZnO@Glu-Safranal NPs leads to a significant reduction in *MMP1* gene expression compared to the control group (0.87-fold, $p = 0.02$) (Fig. 6a). This decrease suggests that the treatment may negatively impact the pathways regulating *MMP1*, which plays a crucial role in extracellular matrix remodeling and tissue repair processes. In addition, the results demonstrate that treatment with ZnO@Glu-Safranal NPs leads to a reduction in *mTOR* gene expression compared to the control group (0.86-fold, $p = 0.03$) (Fig. 6b). This downregulation suggests that the treatment may impact the *mTOR* signaling pathway, which plays a crucial role in regulating various cellular processes, including growth, proliferation, and metabolism. Reduced *mTOR* expressions could have important implications for cellular functions, potentially affecting cell growth and survival.

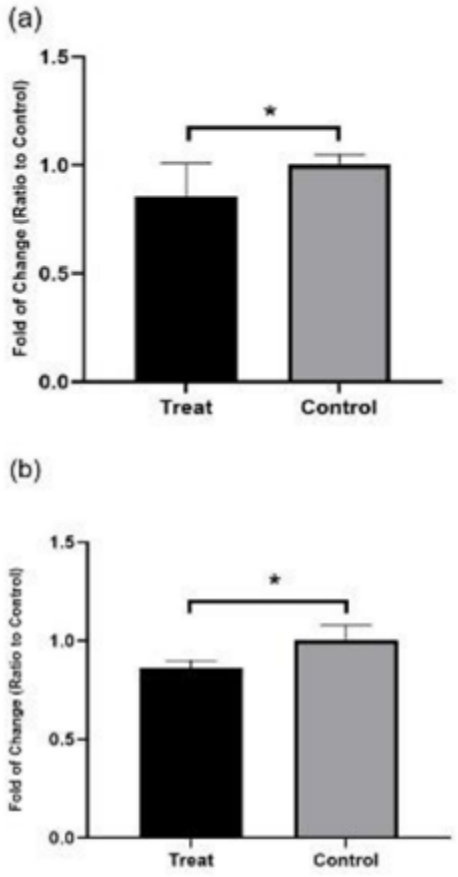

Fig. 6 Impact of ZnO@Glu-Safranal Nanoparticles on the expression of a) *MMP1*; and b) *mTOR* genes in MCF-7 treated cells compared to untreated control cells (n = 3, *= P < 0.05).

Discussion

This study evaluated the impact of zinc oxide nanoparticles conjugated with safranal (ZnO@Glu-Safranal NPs) on the expression of genes involved in cancer progression in the MCF-7 breast cancer cell line. The results showed that treatment with these nanoparticles significantly downregulated the expression of *MMP1* (0.87-fold; $p = 0.02$) and *mTOR* (0.86-fold; $p = 0.03$). These effects suggest a potential role for ZnO@Glu-Safranal NPs in attenuating tumor invasiveness and proliferation by modulating key signaling pathways. These findings directly support our hypothesis that ZnO@Glu-Safranal NPs can modulate cancer-related gene expression by targeting both MMP1 and mTOR, two critical mediators of metastasis and cell proliferation.

The conjugation of safranal to ZnO NPs was confirmed through standard characterization techniques (FT-IR, TEM, and zeta potential analysis), which provide strong evidence for successful chemical binding. However, future research should include quantification of binding efficiency and assessment of nanoparticle stability under physiological conditions to support translational potential.

The downregulation of *MMP1*, a gene closely associated with extracellular matrix degradation and cancer metastasis, supports the hypothesis that these nanoparticles may interfere with the invasive potential of breast cancer cells. This finding aligns with earlier studies. For instance, George et al. (2022) reported that ZnO nanoparticles coated with *Rubus fairholmianus* extract triggered apoptotic pathways in MCF-7 cells, while Ahamed et al. (2011) demonstrated oxidative stress-mediated modulation of gene expression by ZnO NPs in A549 cells. These prior findings reinforce the current results by suggesting that ZnO-based nanoparticles, including our ZnO@Glu-Safranal formulation, may reduce tumor aggressiveness through oxidative and apoptotic pathways involving MMP suppression.

Similarly, Mozdoori et al. (2017) showed that porphyrin-conjugated ZnO nanoparticles influenced the expression of genes associated with non-classical cell death in MCF-7 cells. Bai et al. (2017) found that ZnO NPs caused stress-related protein expression changes using Western blot analysis, and Wang et al. (2020) reported mitochondrial dysfunction and ROS generation

following ZnO NP exposure, although apoptosis markers were unaffected.

The modulation of matrix metalloproteinases (MMPs) by nanoparticles has been reported in several studies. MMPs are typically low in normal tissues but elevated in cancer, contributing to tumor progression (Gonzalez-Avila et al., 2022). For example, Hashimoto et al. (2016) showed that PVP-coated gold and platinum nanoparticles inhibited MMP1 activity in fibroblasts and MMP8/9 in macrophages. Wu et al. (2016) and Zhang et al. (2015) reported reduced MMP2 and MMP9 expression in gastric and squamous carcinoma cells following gold nanoparticle treatment. Conversely, Franková et al. (2016) found that silver nanoparticles increased MMP1 but decreased MMP3 expression in keratinocytes.

Not all nanoparticles suppress MMPs. Liu et al. (2014) showed that citrate-coated gold nanoparticles increased MMP9 in A549 cells, while Pascarelli et al. (2013) found upregulation of MMP1, MMP3, and MMP13 in osteoarthritic chondrocytes treated with PVP-coated NPs. ROS-mediated activation of MMPs by TiO_2, nickel, and cobalt nanoparticles has been described by Wan et al. (2011) and Annangi et al. (2015). Armand et al. (2013) linked TiO_2 NP-induced MMP1 upregulation to IL-1β pathways in human lung fibroblasts. These heterogeneous outcomes highlight the importance of nanoparticle composition and functionalization. The observed *MMP1* downregulation in our study further supports the notion that surface-conjugated agents like safranal can influence the direction of MMP regulation.

In vivo studies show variable outcomes. Park et al. (2010a, 2010b) reported transient MMP induction by Pt and Fe_3O_4 NPs, while Blum et al. (2014) observed persistent MMP9 elevation after CdO NP exposure. Ambalavanan et al. (2013) reported increased MMP9 in neonatal mice exposed to TiO_2 NPs, and Morimoto et al. (2011) found no significant MMP2 changes with NiO NPs. On the other hand, Au and Pt nanoparticles reduced MMP2 and MMP9 expression in diabetic and liver tissues, respectively (Opris et al., 2017; Medhat et al., 2017). Gadolinium metallofullerenol NPs also reduced MMP expression and inhibited tumor growth (Kang et al., 2012).

These findings illustrate the complexity of NP effects on MMP regulation, which can vary depending on NP size, composition, surface chemistry, and cellular context. The underlying mechanisms are still under investigation, but proposed explanations include direct NP-MMP interactions or modulation through ROS and inflammatory pathways. Our findings contribute to this growing body of evidence by showing that ZnO@Glu-Safranal NPs selectively suppress *MMP1*, potentially through antioxidant and anti-inflammatory actions of safranal, warranting further mechanistic studies.

mTOR is another critical signaling molecule involved in cell growth, metabolism, and survival (Saxton and Sabatini, 2017). Aberrant mTOR activity is common in cancer, making it an important therapeutic target. Compared to conventional chemotherapies, mTOR inhibitors generally exhibit better tolerability (Hua et al., 2019). Several NPs have been shown to modulate mTOR: inhibitory effects have been reported for iron oxide (Khan et al., 2012), zinc oxide (Roy et al., 2014), TiO_2 (Zhang et al., 2016), and bismuth NPs (Liu et al., 2018), while copper oxide (Edelmann et al., 2014) and gold NPs (Wang et al., 2012) activate mTOR. Our findings of mTOR downregulation are in line with previous reports of NP-induced mTOR suppression, suggesting that ZnO@Glu-Safranal NPs may interfere with cancer cell metabolism and survival signaling.

Despite these findings, the precise mechanisms by which NPs influence mTOR remain unclear. Recent work challenges the "proton sponge" hypothesis and instead points to the involvement of lysosomes in NP-induced signaling (Lunova et al., 2019). Sub-cytotoxic NP exposure may cause oxidative stress and disrupt organelles such as lysosomes and mitochondria, linking cellular stress responses with mTOR modulation. Further studies are required to unravel these dynamics and understand their implications in cancer therapy. Given the known antioxidant properties of safranal, it is plausible that ZnO@Glu-Safranal NPs reduce mTOR activity by attenuating oxidative stress, which merits further investigation in future mechanistic studies.

Study Limitations

This study focused on evaluating changes in the mRNA expression levels of *MMP1* and *mTOR* in response to ZnO@Glu-Safranal nanoparticles but did not include functional validation assays such as Western blotting, apoptosis assays, or assessments of long-term effects on cellular metabolism.

Additionally, control groups treated with individual ZnO nanoparticles or safranal alone were not included, which limits the ability to distinguish their independent contributions to gene expression changes. Despite these limitations, the study was designed as a preliminary investigation to provide initial insights into the gene-level effects of the conjugated nanoparticles on cancer-related pathways. Future studies are encouraged to incorporate protein-level validation, functional assays, and comparative groups to more comprehensively assess the biological impact and therapeutic potential of these nanoparticles.

Conclusions

This study demonstrates that ZnO nanoparticles conjugated with Safranal (ZnO@Glu-Safranal) significantly modulate the expression of key regulatory genes involved in tumor metabolism and progression in MCF-7 breast cancer cells. Notably, the treatment resulted in downregulation of *MMP1* and *mTOR*, which may indicate a reduction in metastatic potential and metabolic activity. These findings underscore the therapeutic potential of combining nanotechnology with natural bioactive compounds such as Safranal. However, due to resource limitations, functional assays to confirm these gene expression changes at the protein or cellular level were not performed, and this represents a limitation of the current study. Further in-depth studies are warranted to elucidate the molecular pathways involved and to assess the clinical relevance of ZnO@Glu-Safranal in cancer therapy.

Acknowledgements

Not applicable.

Author Contributions

R.J.: Formal analysis, Investigation, Resources, Data Curation; A.J.: Conceptualization, Methodology, Validation, Writing - Original Draft, Writing - Review & Editing, Supervision, Project administration; S.A.S.S.: Methodology, Validation; A.S.: Formal analysis, Conceptualization, Methodology, Validation, Supervision, Project administration; L.K.: Investigation, Resources. All authors have provided their approval for the final version of the manuscript.

Funding

This research did not receive any specific funding from public, commercial, or non-profit funding agencies.

Data Availability

All data generated or analyzed during this study are included in this paper

Ethical Approval

Not applicable.

Competing Interests

The authors declare that there are no conflicts of interest.

Research Involving Humans and Animals Statement None.

Conflict of Interest

The authors declare no conflicts of interest

References

Abdalla, Y., Abdalla, A., Hamza, A.A., Amin, A., 2022. Safranal Prevents Liver Cancer Through Inhibiting Oxidative Stress and Alleviating Inflammation. Front. Pharmacol. 12, 777500. https://doi.org/10.3389/fphar.2021.777500

Ahamed, M., Akhtar, M.J., Raja, M., Ahmad, I., Siddiqui, M.K., AlSalhi, M.S., Alrokayan, S., 2011. ZnO nanorod-induced apoptosis in human alveolar adenocarcinoma cells via p53, survivin and bax/bcl-2 pathways: role of oxidative stress. Nanomedicine 7(6), 904–913. https://doi.org/10.1016/j.nano.2011.04.011

Al-Thani, A.N., Jan, A.G., Abbas, M., Geetha, M., Sadasivuni, K.K., 2024. Nanoparticles in cancer theragnostic and drug delivery: A comprehensive review. Life Sci. 352, 122899. https://doi.org/10.1016/j.lfs.2024.122899

Ambalavanan, N., Stanishevsky, A., Bulger, A., Halloran, B., Steele, C., Vohra, Y., Matalon, S., 2013. Effect of nanoparticles on lung inflammation. Am. J. Physiol. Lung Cell Mol. Physiol. 304, L152. https://doi.org/10.1152/ajplung.00013.2012

Anjum, S., Hashim, M., Malik, S.A., Khan, M., Lorenzo, J.M., Abbasi, B.H., Hano, C., 2021. Recent Advances in Zinc Oxide Nanoparticles (ZnO NPs) for Cancer Diagnosis, Target Drug Delivery, and Treatment. Cancers 13(18), 4570. https://doi.org/10.3390/cancers13184570

Annangi, B., Bach, J., Vales, G., Rubio, L., Marcos, R., Hernández, A., 2015. Long-term exposures to low doses of cobalt nanoparticles induce cell transformation enhanced by oxidative damage. Nanotoxicology 9(2), 138-147. https://doi.org/10.3109/17435390.2014.900582

Armand, L., Dagouassat, M., Belade, E., Simon-Deckers, A., Le Gouvello, S., Tharabat, C., Duprez, C., Andujar, P., Pairon, J.C., Boczkowski, J., Lanone, S., 2013. Titanium dioxide nanoparticles induce

matrix metalloprotease 1 in human pulmonary fibroblasts partly via an interleukin-1β-dependent mechanism. Am. J. Respir. Cell Mol. Biol. 48(3), 354-363. https://doi.org/10.1165/rcmb.2012-0099OC

Bai, D.P., Zhang, X.F., Zhang, G.L., Huang, Y.F., Gurunathan, S., 2017. Zinc oxide nanoparticles induce apoptosis and autophagy in human ovarian cancer cells. Int. J. Nanomed. 12, 6521–6535. https://doi.org/10.2147/IJN.S140071

Blum, J.L., Rosenblum, L.K., Grunig, G., Beasley, M.B., Xiong, J.Q., Zelikoff, J.T., 2014. Inhalation toxicity of nanoparticles in lung tissue. Inhal. Toxicol. 26, 48. https://doi.org/10.3109/08958378.2013.851746

Edelmann, M.J., Shack, L.A., Naske, C.D., Walters, K.B., Nanduri, B., 2014. Proteomic analysis of cellular responses to nanoparticles. PLoS One 9, e114390. https://doi.org/10.1371/journal.pone.0114390

Ezhuthupurakkal, P.B., Ariraman, S., Arumugam, S., Subramaniyan, N., Muthuvel, S.K., Kumpati, P., Rajamani, B., Chinnasamy, T., 2018. Anticancer potential of ZnO nanoparticle-ferulic acid conjugate on Huh-7 and HepG2 cells and diethyl nitrosamine induced hepatocellular cancer on Wistar albino rat. Nanomedicine 14(2), 415–428. https://doi.org/10.1016/j.nano.2017.11.003

Franková, J., Pivodová, V., Vágnerová, H., Juráňová, J., Ulrichová, J., 2016. Effects of silver nanoparticles on primary cell cultures of fibroblasts and keratinocytes in a wound-healing model. J. Appl. Biomater. Funct. Mater. 14(2), e137–e142. https://doi.org/10.5301/jabfm.5000268

George, B.P., Rajendran, N.K., Houreld, N.N., Abrahamse, H., 2022. Rubus capped zinc oxide nanoparticles induce apoptosis in MCF-7 breast cancer cells. Molecules 27(20), 6862. https://doi.org/10.3390/molecules27206862

Gonzalez-Avila, G., Sommer, B., García-Hernandez, A.A., Ramos, C., Flores-Soto, E., 2022. Nanotechnology and matrix metalloproteinases in cancer diagnosis and treatment. Front. Mol. Biosci. 9, 918789. https://doi.org/10.3389/fmolb.2022.918789

Hashimoto, M., Yamaguchi, S., Sasaki, J., Kawai, K., Kawakami, H., Iwasaki, Y., Imazato, S., 2016. Inhibition of matrix metalloproteinases and toxicity of gold and platinum nanoparticles in L929 fibroblast cells. Eur. J. Oral Sci. 124(1), 68–74. https://doi.org/10.1111/eos.12235

Hua, H., Kong, Q., Zhang, H., Wang, J., Luo, T., Jiang, Y., 2019. Regulation of tumor biology by signaling pathways. J. Hematol. Oncol. 12, 71. https://doi.org/10.1186/s13045-019-0754-1

Kang, S.G., Zhou, G., Yang, P., Liu, Y., Sun, B., Huynh, T., Meng, H., Zhao, L., Xing, G., Chen, C., Zhao, Y., Zhou, R., 2012. Computational study of nanoparticle interactions. Proc. Natl. Acad. Sci. USA 109, 15431. https://doi.org/10.1073/pnas.1204600109

Khan, M.I., Mohammad, A., Patil, G., Naqvi, S.A., Chauhan, L.K., Ahmad, I., 2012. Toxicity evaluation of biomaterials. Biomaterials 33, 1477. https://doi.org/10.1016/j.biomaterials.2011.10.080

Li, Z., Guo, D., Yin, X., Ding, S., Shen, M., Zhang, R., Wang, Y., Xu, R., 2020. Zinc oxide nanoparticles induce human multiple myeloma cell death via reactive oxygen species and Cyt-C/Apaf-1/Caspase-9/Caspase-3 signaling pathway in vitro. Biomed. Pharmacother. 122, 109712. https://doi.org/10.1016/j.biopha.2019.109712

Liu, J., Li, H.Q., Zhou, F.X., Yu, J.W., Sun, L., Han, Z.H., 2017. Targeting the mTOR pathway in breast cancer. Tumour Biol. 39(6), 1010428317710825. https://doi.org/10.1177/1010428317710825

Liu, Y., Yu, H., Zhang, X., Wang, Y., Song, Z., Zhao, J., Shi, H., Li, R., Wang, Y., Zhang, L.W., 2018. Evaluation of nanoparticle safety in biological systems. Nanotoxicology 12, 586. https://doi.org/10.1080/17435390.2018.1466932

Liu, Z., Wu, Y., Guo, Z., Liu, Y., Shen, Y., Zhou, P., Lu, X., 2014. Effects of internalized gold nanoparticles with respect to cytotoxicity and invasion activity in lung cancer cells. PLoS One 9(6), e99175. https://doi.org/10.1371/journal.pone.0099175

Lunova, M., Smolková, B., Lynnyk, A., Uzhytchak, M., Jirsa, J., Kubinová, Š., Dejneka, A., Lunov, O., 2019. Nanoparticle-mediated cancer therapies. Cancers 11, 82. https://doi.org/10.3390/cancers11010082

Malaekeh-Nikouei, B., Mousavi, S.H., Shahsavand, S., Mehri, S., Nassirli, H., Moallem, S.A., 2013. Assessment of cytotoxic properties of safranal and nanoliposomal safranal in various cancer cell lines. Phytother. Res. 27(12), 1868–1873. https://doi.org/10.1002/ptr.4945

Medhat, A., Mansour, S., El-Sonbaty, S., Kandil, E., Mahmoud, M., 2017. Role of nanoparticles in tumor biology. Tumour Biol. 39, 1010428317717259. https://doi.org/10.1177/1010428317717259

Mishra, P., Ahmad, A., Al-Keridis, L.A., Alshammari, N., Alabdallah, N.M., Muzammil, K., Saeed, M., Ansari, I.A., 2022. Doxorubicin-Conjugated Zinc Oxide Nanoparticles, Biogenically Synthesised Using a Fungus Aspergillus niger, Exhibit High Therapeutic Efficacy against Lung Cancer Cells. Molecules 27(8), 2590. https://doi.org/10.3390/molecules27082590

Mishra, P., Ahmad, M.F.A., Al-Keridis, L.A., Saeed, M., Alshammari, N., Alabdallah, N.M., Tiwari, R.K., Ahmad, A., Verma, M., Fatima, S., Ansari, I.A., 2024.

Corrigendum: Methotrexate-conjugated zinc oxide nanoparticles exert substantially improved cytotoxic effect on lung cancer cells by inducing apoptosis. Front. Pharmacol. 15, 1423402. https://doi.org/10.3389/fphar.2024.1423402

Mohamed, S.Y., Elshoky, H.A., El-Sayed, N.M., Fahmy, H.M., Ali, M.A., 2024. Ameliorative effect of zinc oxide-chitosan conjugates on the anticancer activity of cisplatin: Approach for breast cancer treatment. Int. J. Biol. Macromol. 257(Pt 1), 128597. https://doi.org/10.1016/j.ijbiomac.2023.128597

Morimoto, Y., Oyabu, T., Ogami, A., Myojo, T., Kuroda, E., Hirohashi, M., Shimada, M., Lenggoro, W., Okuyama, K., Tanaka, I., 2011. Safety assessment of nanoparticles in occupational environments. Ind. Health 49, 344. https://doi.org/10.2486/indhealth.MS1218

Mozdoori, N., Safarian, S., Sheibani, N., 2017. Augmentation of the cytotoxic effects of zinc oxide nanoparticles by MTCP conjugation: Non-canonical apoptosis and autophagy induction in human adenocarcinoma breast cancer cell lines. Mater. Sci. Eng. C 78, 949–959. https://doi.org/10.1016/j.msec.2017.03.300

Naghshineh, A., Dadras, A., Ghalandari, B., Riazi, G.H., Modaresi, S.M., Afrasiabi, A., Aslani, M.K., 2015. Safranal as a novel anti-tubulin binding agent with potential use in cancer therapy: An in vitro study. Chem.-Biol. Interact. 238, 151–160. https://doi.org/10.1016/j.cbi.2015.06.023

Opris, R., Tatomir, C., Olteanu, D., Moldovan, R., Moldovan, B., David, L., Nagy, A., Decea, N., Kiss, M.L., Filip, G.A., 2017. Effects of nanostructured materials on cellular response. Colloids Surf. B Biointerfaces 150, 192. https://doi.org/10.1016/j.colsurfb.2016.11.033

Park, E.J., Kim, H., Kim, Y., Park, K., 2010a. Intratracheal instillation of platinum nanoparticles may induce inflammatory responses in mice. Arch. Pharm. Res. 33(5), 727-735. https://doi.org/10.1007/s12272-010-0512-y

Park, E.J., Kim, H., Kim, Y., Yi, J., Choi, K., Park, K., 2010b. Inflammatory responses may be induced by a single intratracheal instillation of iron nanoparticles in mice. Toxicology 275(1-3), 65-71. https://doi.org/10.1016/j.tox.2010.06.002

Pascarelli, N.A., Moretti, E., Terzuoli, G., Lamboglia, A., Renieri, T., Fioravanti, A., Collodel, G., 2013. Effects of gold and silver nanoparticles in cultured human osteoarthritic chondrocytes. J. Appl. Toxicol. 33(12), 1506-1513. https://doi.org/10.1002/jat.2912

Puente, X.S., Sánchez, L.M., Overall, C.M., López-Otín, C., 2003. Human and mouse proteases: a comparative genomic approach. Nat. Rev. Genet. 4, 544–558. https://doi.org/10.1038/nrg1111

Roy, R., Singh, S.K., Chauhan, L.K., Das, M., Tripathi, A., Dwivedi, P.D., 2014. Cellular response to toxic nanoparticles. Toxicol. Lett. 227, 29. https://doi.org/10.1016/j.toxlet.2014.02.024

Rudolph, A., Chang-Claude, J., Schmidt, M.K., 2016. Gene-environment interaction and risk of breast cancer. Br. J. Cancer 114, 125–133. https://doi.org/10.1038/bjc.2015.439

Samarghandian, S., Shoshtari, M.E., Sargolzaei, J., Hossinimoghadam, H., Farahzad, J.A., 2014. Anti-tumor activity of safranal against neuroblastoma cells. Pharmacogn. Mag. 10(Suppl 2), S419–S424. https://doi.org/10.4103/0973-1296.133296

Saxton, R.A., Sabatini, D.M., 2017. mTOR signaling in cancer. Cell 168, 960. https://doi.org/10.1016/j.cell.2017.02.004

Sirelkhatim, A., Mahmud, S., Seeni, A., Kaus, N.H.M., Ann, L.C., Bakhori, S.K.M., Hasan, H., Mohamad, D., 2015. Review on Zinc Oxide Nanoparticles: Antibacterial Activity and Toxicity Mechanism. Nano-Micro Lett. 7(3), 219–242. https://doi.org/10.1007/s40820-015-0040-x

Tajmehri, H., Mousavi, F.S., Heydarnezhad, M., Golrokh, F.J., Nezami, P.V., Khanpour, P., Ghafardoust Noroudi, S., Salehzadeh, A., 2024. Evaluation of the cytotoxic effect of cobalt oxide nanoparticles functionalized by glucose and conjugated with lapatinib (Co3O4@Glu-Lapatinib) on a lung cancer cell line and evaluation of the expression of CASP8, mTOR1, and MAPK1 genes. BioNanoScience 14, 999–1010. https://doi.org/10.1007/s12668-024-01348-6

Wang, B., Chen, N., Wei, Y., Li, J., Sun, L., Wu, J., Huang, Q., Liu, C., Fan, C., Song, H., 2012. Functional properties of nanomaterials in biological systems. Sci. Rep. 2, 563. https://doi.org/10.1038/srep00563

Wang, J., Chen, Y., Lu, D., Chen, Y., Jia, Y., Ying, X., Xiong, H., Zhao, W., Zhou, J., Wang, L., 2017. Matrix metalloproteinase-1 expression in breast carcinoma: a marker for unfavorable prognosis. Oncotarget 8, 91379–91390. https://doi.org/10.18632/oncotarget.20557

Wang, J., Deng, X., Zhang, F., Chen, D., Ding, W., 2014. ZnO nanoparticle-induced oxidative stress triggers apoptosis by activating JNK signaling pathway in cultured primary astrocytes. Nanoscale Res. Lett. 9, 117. https://doi.org/10.1186/1556-276X-9-117

Wang, S.W., Lee, C.H., Lin, M.S., Chi, C.W., Chen, Y.J., Wang, G.S., Liao, K.W., Chiu, L.P., Wu, S.H., Huang, D.M., Chen, L., Shen, Y.S., 2020. ZnO nanoparticles induced caspase-dependent apoptosis in gingival squamous cell carcinoma through mitochondrial dysfunction and p70S6K signaling pathway. Int. J. Mol. Sci. 21(5), 1612. https://doi.org/10.3390/ijms21051612

Wan, R., Mo, Y., Chien, S., Li, Y., Tollerud, D.J., Zhang, Q., 2011. The role of hypoxia inducible factor-1α in the increased MMP-2 and MMP-9 production by human monocytes exposed to nickel nanoparticles. Nanotoxicology 5(4), 568-582. https://doi.org/10.3109/17435390.2010.537791

Wu, Y., Zhang, Q., Ruan, Z., Yin, Y., 2016. Intrinsic effects of gold nanoparticles on proliferation and invasion activity in SGC-7901 cells. Oncol. Rep. 35(3), 1457-1462. https://doi.org/10.3892/or.2015.4474

Zhang, Y., Chen, W., Wang, S., Liu, Y., Pope, C., 2008. Phototoxicity of zinc oxide nanoparticle conjugates in human ovarian cancer NIH: OVCAR-3 cells. J. Biomed. Nanotechnol. 4, 432–438. https://doi.org/10.1166/jbn.2008.006

Zhang, Q., Ma, Y., Yang, S., Xu, B., Fei, X., 2015. Small-sized gold nanoparticles inhibit the proliferation and invasion of SW579 cells. Mol. Med. Rep. 12(6), 8313-8319. https://doi.org/10.3892/mmr.2015.4433

Zhang, X., Yin, H., Li, Z., Zhang, T., Yang, Z., 2016. Molecular mechanisms of nanoparticle-induced cytotoxicity. Cell Biol. Toxicol. 32, 513. https://doi.org/10.1007/s10565-016-9352-y